Supporting Information

Isomerization design for improving the efficiency of red thermally activated delayed fluorescence emitters based on pyridopyrazinophenanthroline acceptor

Guo Yuan[1,†], Da-Hao Wang [1,†], Feng-Ming Xie[2], Bo Zhang[1], Ying-Yuan Hu[1], Qiang Zhang[1], Hao-Ze Li[3], Yan-Qing Li[3,*], Jian-Xin Tang[2,*] and Xin Zhao[1,*]

1. School of chemistry and Life Sciences, Suzhou University of Science and Technology, Suzhou, Jiangsu, 215009, China.

2. Jiangsu Key Laboratory for Carbon-Based Functional Materials & Devices, Institute of Functional Nano & Soft Materials (FUNSOM), Soochow University, Suzhou, Jiangsu, 215123, China.

3. School of Physics and Electronic Science, East China Normal University, Shanghai, 200062, China

† These authors contributed equally to this work.

*Corresponding authors:

Xin Zhao, Email: zhaoxinsz@usts.edu.cn *(X. Zhao)*

Jian-Xin Tang, Email: jxtang@suda.edu.cn *(J.X. Tang)*

Yan-Qing Li, Email: yqli@phy.ecnu.edu.cn *(Y.Q. Li)*

Experimental Section

General information

All the reagents were purchased from commercial sources and used without further purification. All the reactions were performed under nitrogen atmosphere, and the crude products were purified by column chromatography before material characterizations and device fabrication. Chemical structures were determined by ^{1}H and ^{13}C nuclear magnetic resonance (NMR) spectra with a Bruker AVANCE III type 400 MHz NMR Spectrometer in $CDCl_3$ solution, and ultrafleXtreme MALDI-TOF mass spectrometry. Ultraviolet-visible absorption spectra were recorded at room temperature with a Perkin-Elmer Lambda 750 UV-Vis spectrophotometer. Optical bandgap (E_g) was determined from the onset of the absorption spectra. Low-temperature fluorescence and phosphorescence spectra were measured with a FLS 920 spectrometer (Einburgh Corporation) in toluene at 77 K. Transient PL decay curves of the films were measured with a Quantaurus-Tau fluorescence lifetime spectrometer (C11367-32, Hamamatsu Photonics) with an excitation wavelength of 365 nm under vacuum atmosphere. Cyclic voltammetry (CV) measurements were conducted on a RST 3100 electrochemical work station. A platinum disk was used as the working electrode, glassy carbon was used as the counter electrode, Ag/AgCl was used as the reference electrode, tetrabutylammonium hexafluorophosphate was used as the electrolyte, and ferrocene was used as the internal standard. Thermal gravimetric analysis (TGA) curve in the range of 50-700 °C was conducted at a heating rate of 10 °C/min in a nitrogen atmosphere with a HCT-2 instrument.

Device fabrication and measurements

OLEDs were fabricated on the patterned indium-tin-oxide (ITO)-coated glass substrates with a sheet resistance of ~15 Ω per square. The ITO-coated glass substrates were successively cleaned in ultrasonic baths with acetone, ethanol, and deionized water, and then dried in an oven at 110 °C. The ITO-coated glass substrates were transferred into a high-vacuum deposition chamber (base pressure $\leq 2\times10^{-6}$ mbar) for the thermal deposition of organic materials and metal electrodes through shadow masks. Layer thickness and deposition rate were monitored by an oscillating quartz thickness monitor. The active area of OLEDs was defined to be 10 mm^2. The fabricated devices were transferred to an interconnected nitrogen-filled glovebox for the encapsulation with a glass cap and epoxy glue. Current density-voltage-luminance (J-V-L) characteristics and EL spectra of the devices were measured simultaneously with a source meter (Keithley model 2400) and a luminance meter/spectrometer (PhotoResearch PR670). The CIE 1931 color coordinates were obtained from the EL spectra. The EQE values were calculated by assuming an ideal Lambertian emission profile, which were verified by the independent measurements of luminous flux with an integrating sphere (Hamamatsu Photonics K.K. C9920-12).

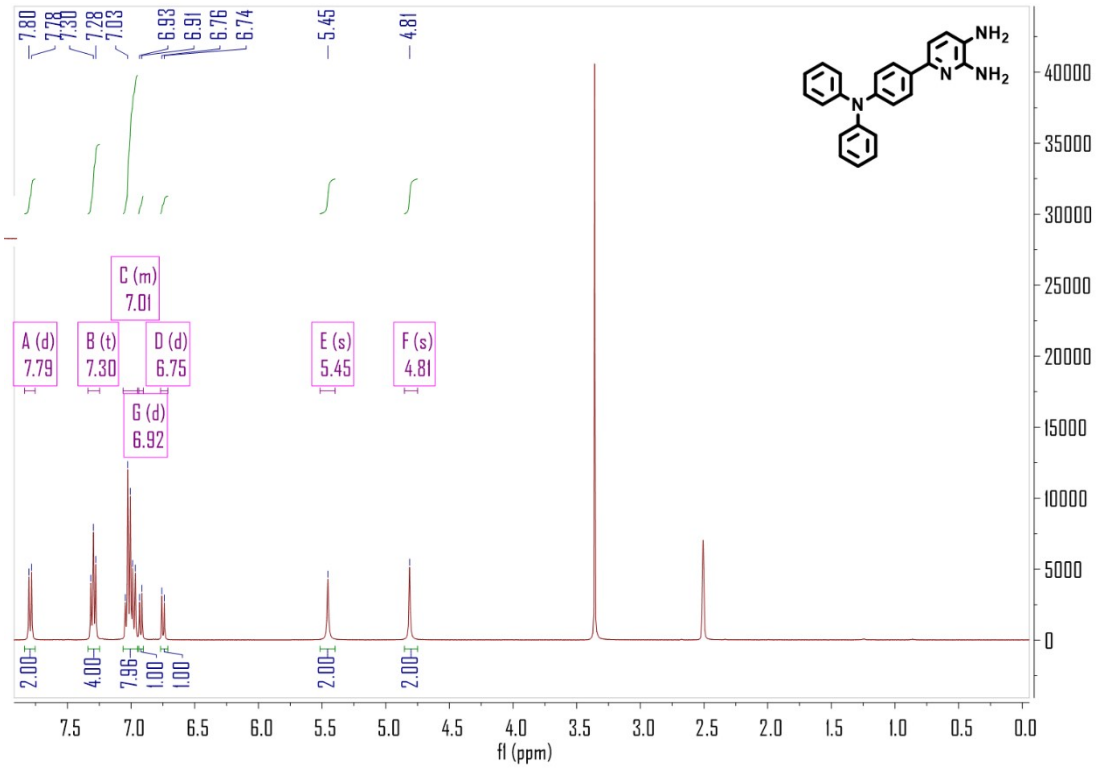

Figure S1. ^{1}H NMR spectrum of oTPA-B (400 MHz, *d*-DMSO).

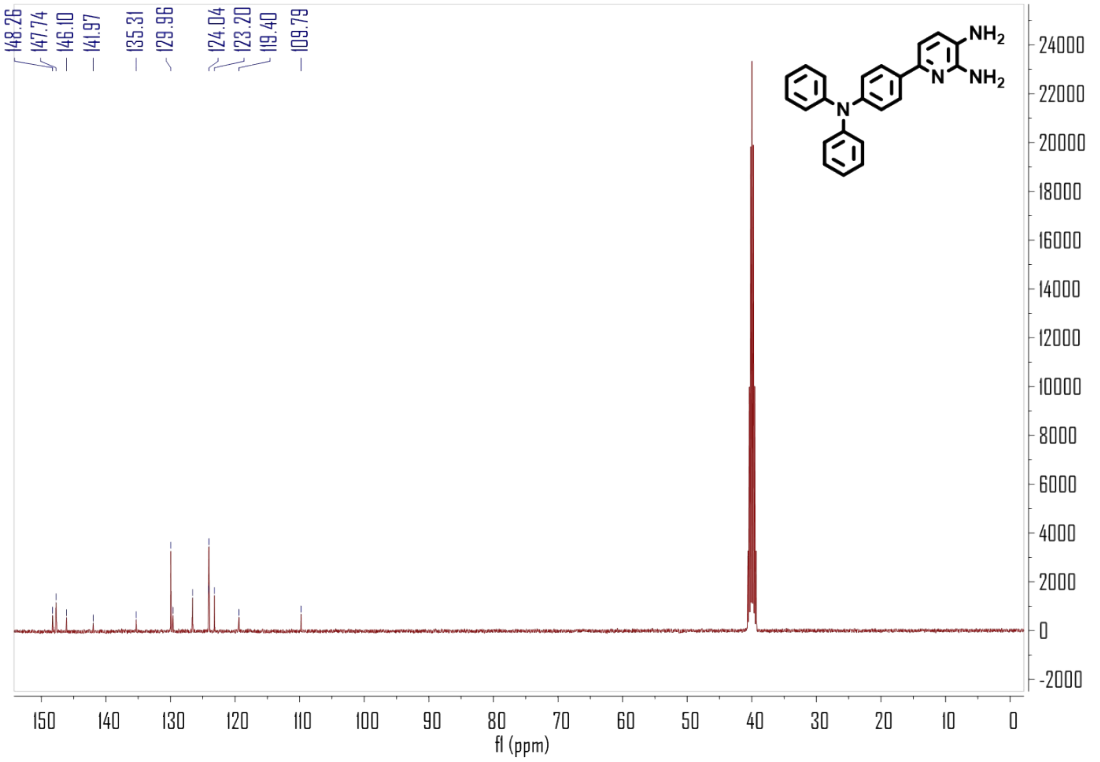

Figure S2. ^{13}C NMR spectrum of oTPA-B (400 MHz, *d*-DMSO).

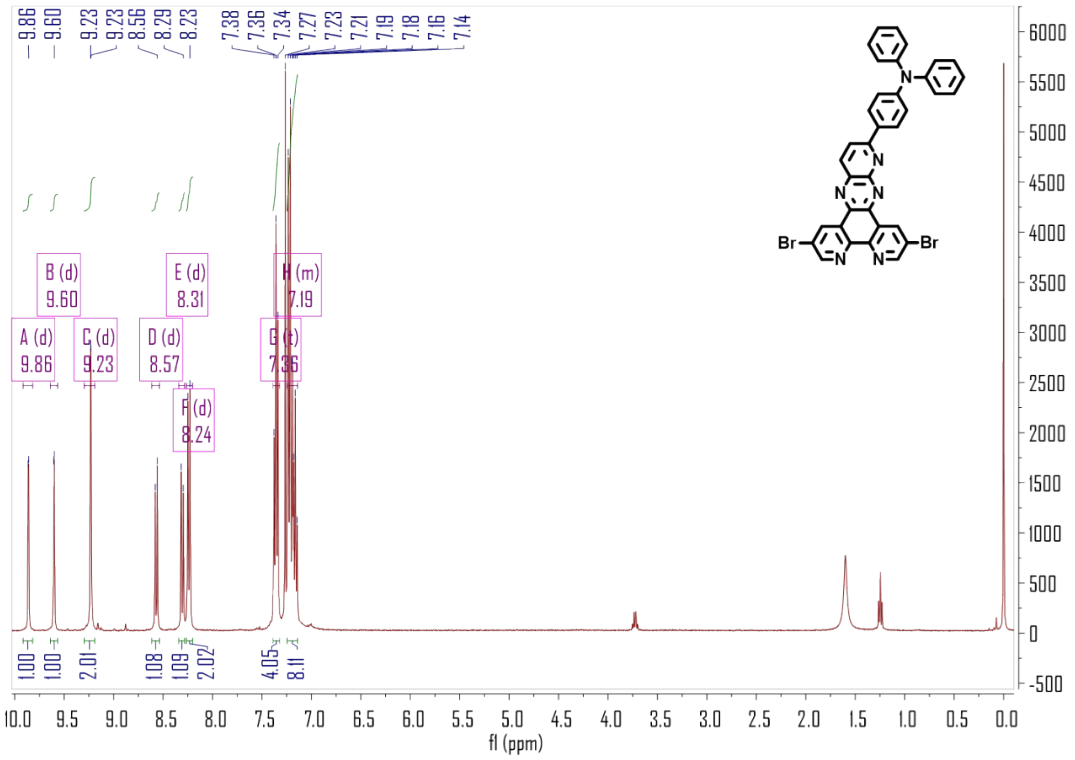

Figure S3. ^{1}H NMR spectrum of oTPA-PPP-2Br (400 MHz, $CDCl_3$).

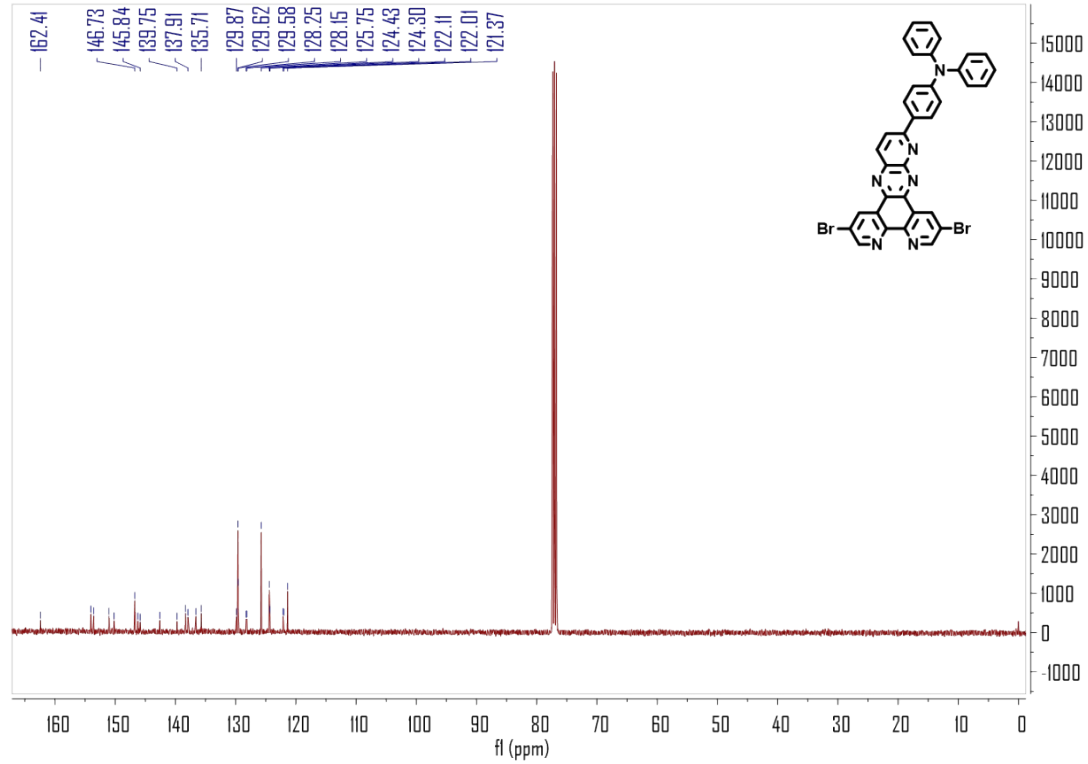

Figure S4. ^{13}C NMR spectrum of oTPA-PPP-2Br (400 MHz, $CDCl_3$).

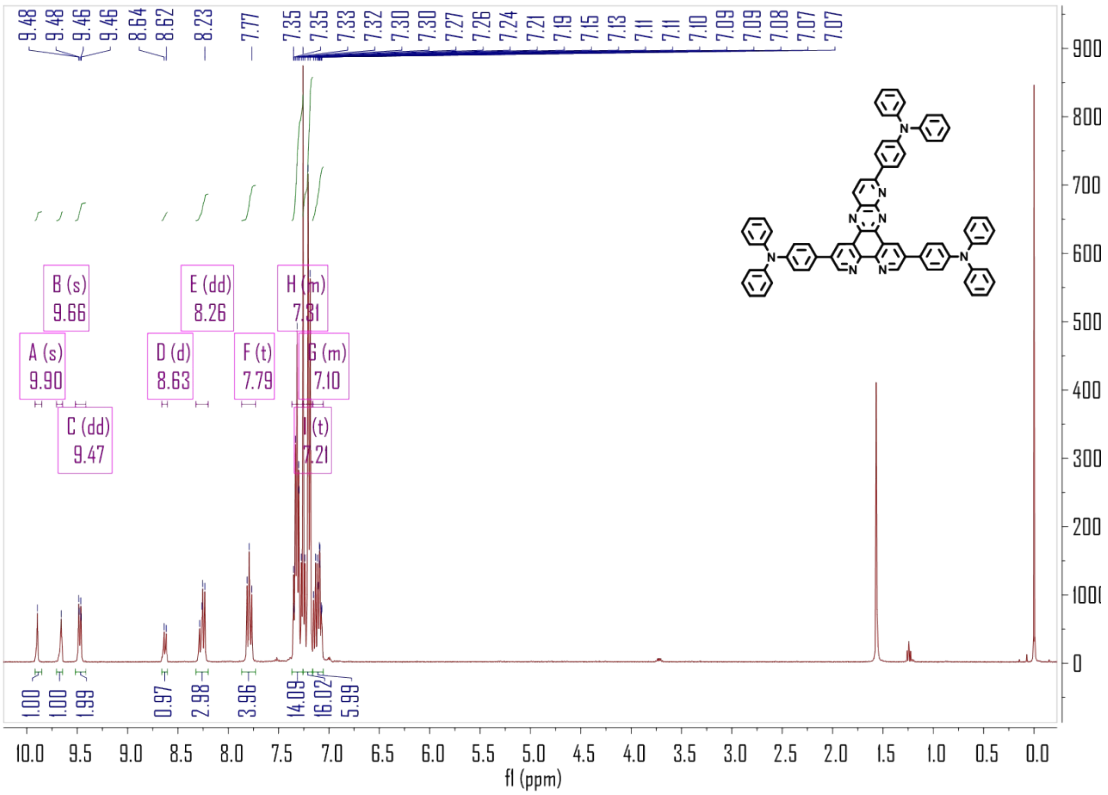

Figure S5. ^{1}H NMR spectrum of otriTPA-PPP (400 MHz, $CDCl_3$).

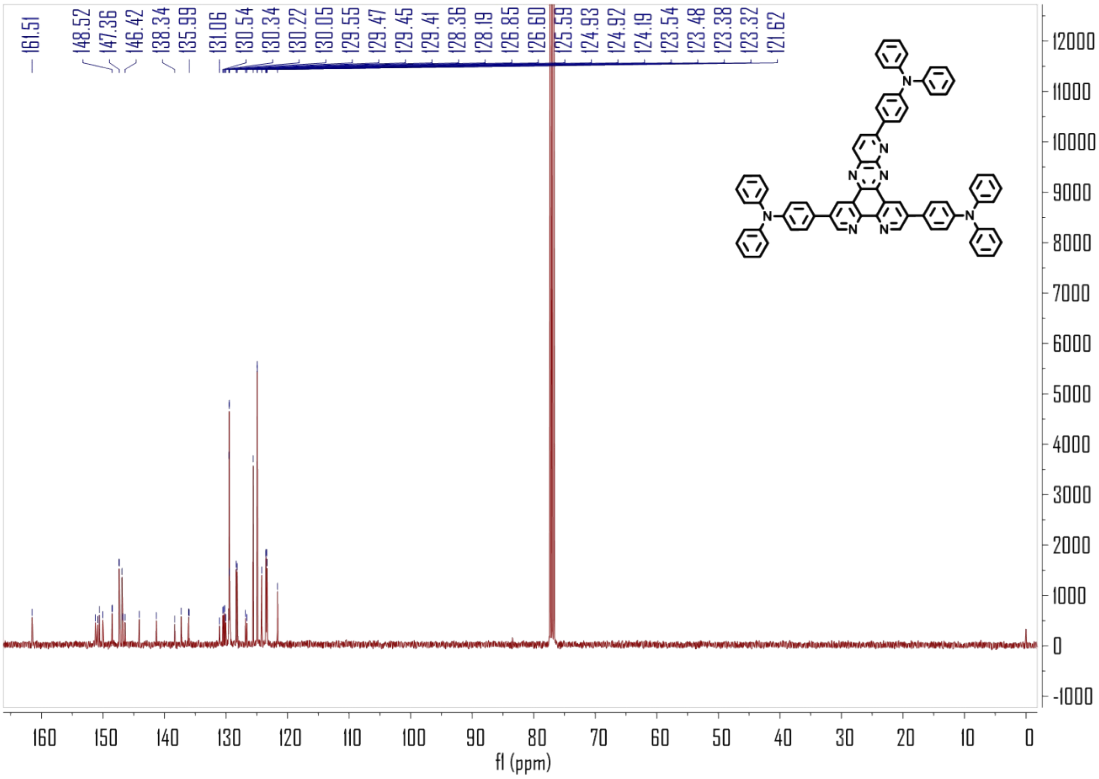

Figure S6. ^{13}C NMR spectrum of otriTPA-PPP (400 MHz, $CDCl_3$).

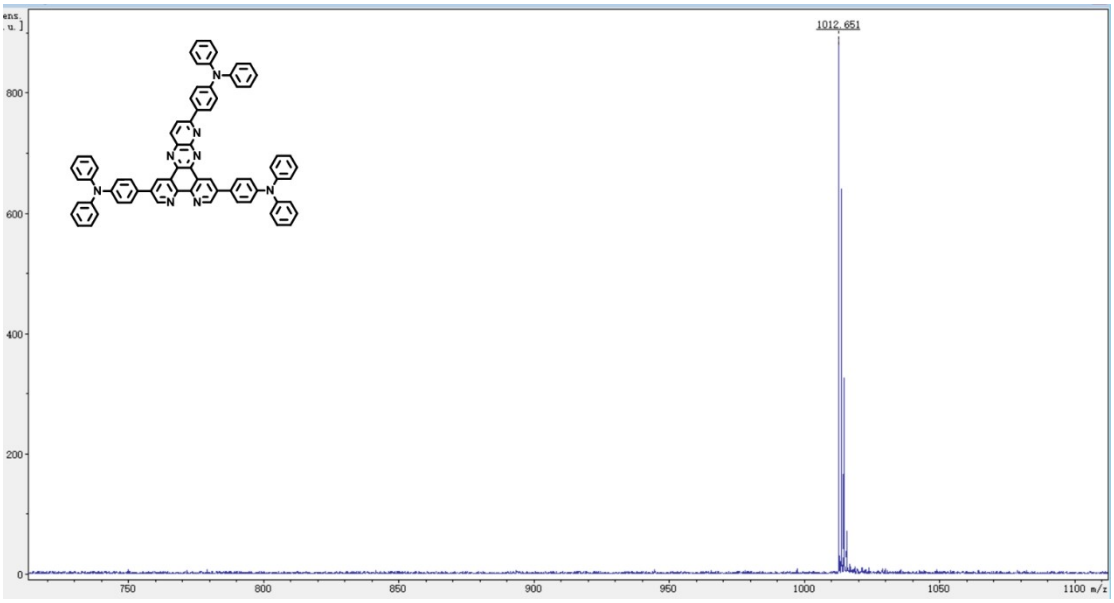

Figure S7. MALDI-TOF MS spectrum of otriTPA-PPP.

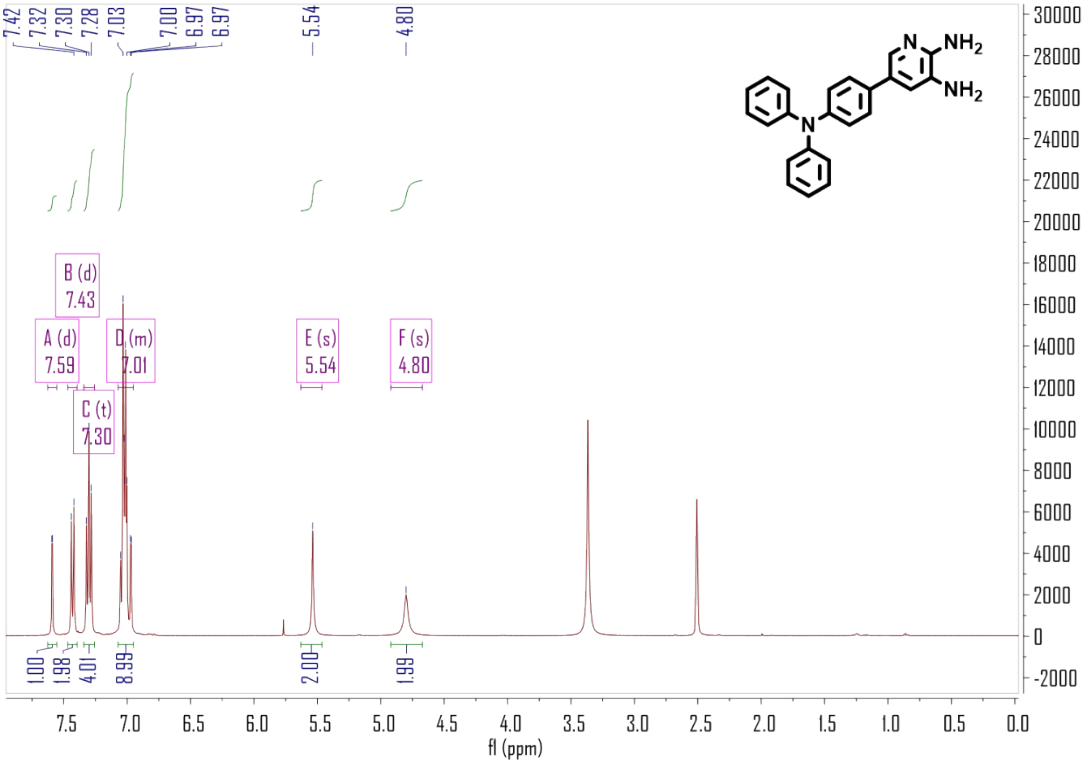

Figure S8. ^{1}H NMR spectrum of mTPA-B (400 MHz, *d*-DMSO).

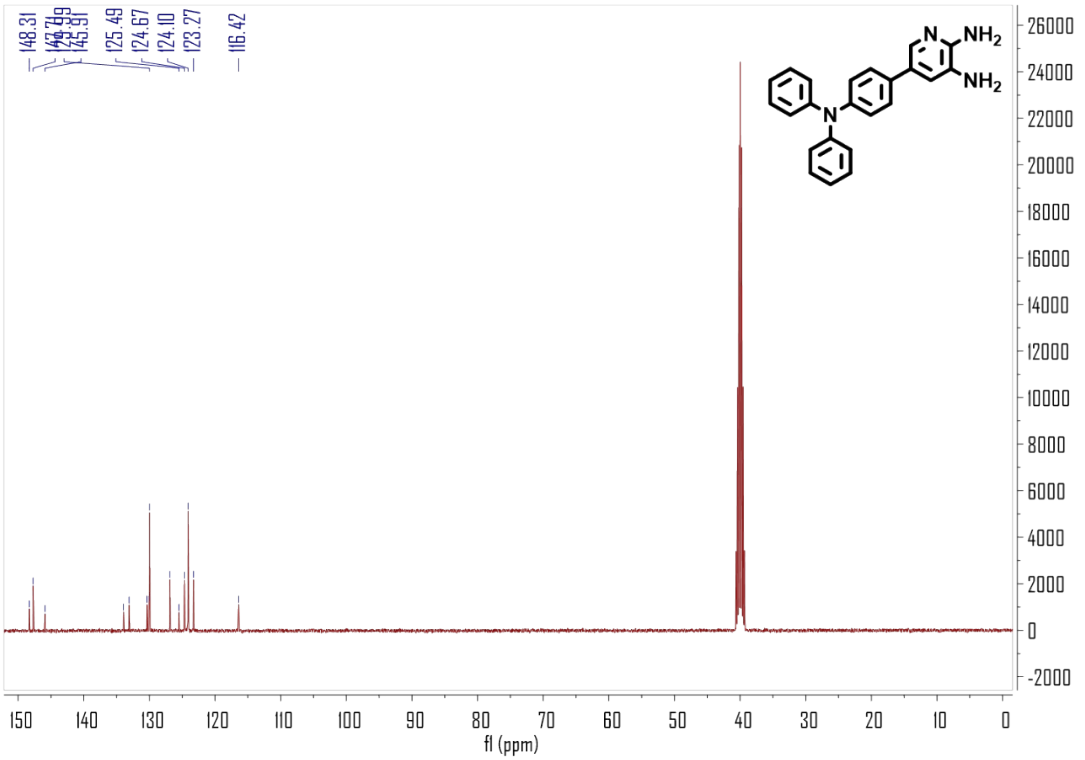

Figure S9. ^{13}C NMR spectrum of mTPA-B (400 MHz, *d*-DMSO).

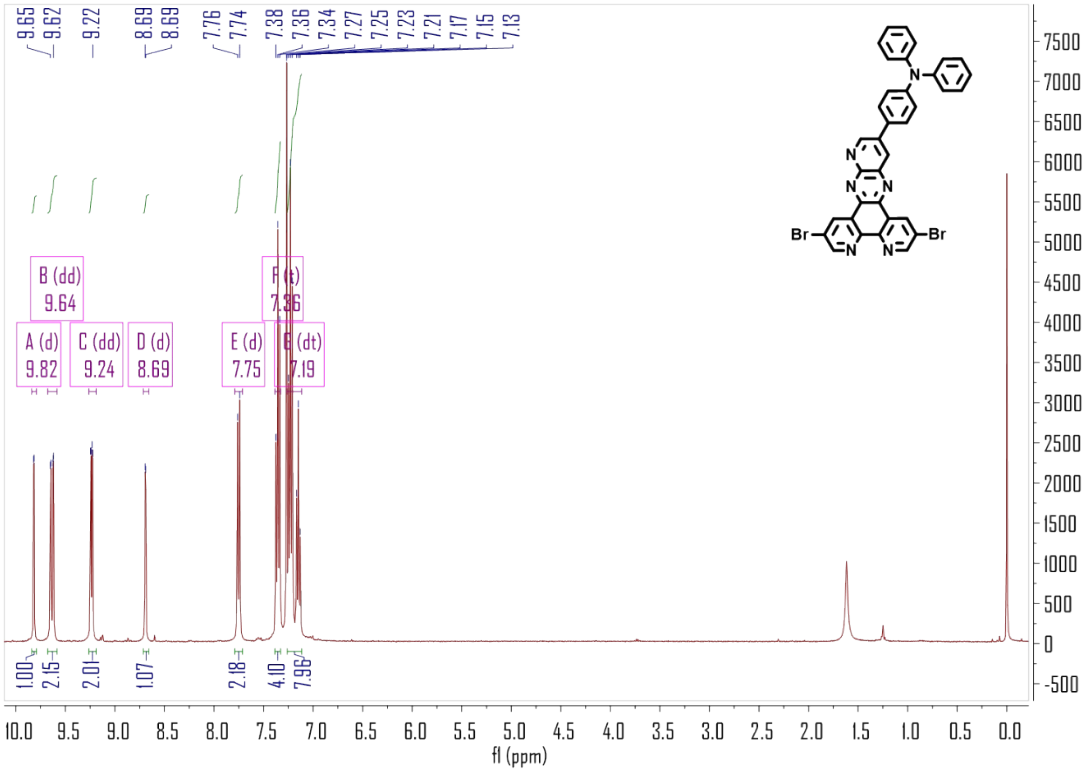

Figure S10. ^{1}H NMR spectrum of mTPA-PPP-2Br (400 MHz, $CDCl_3$).

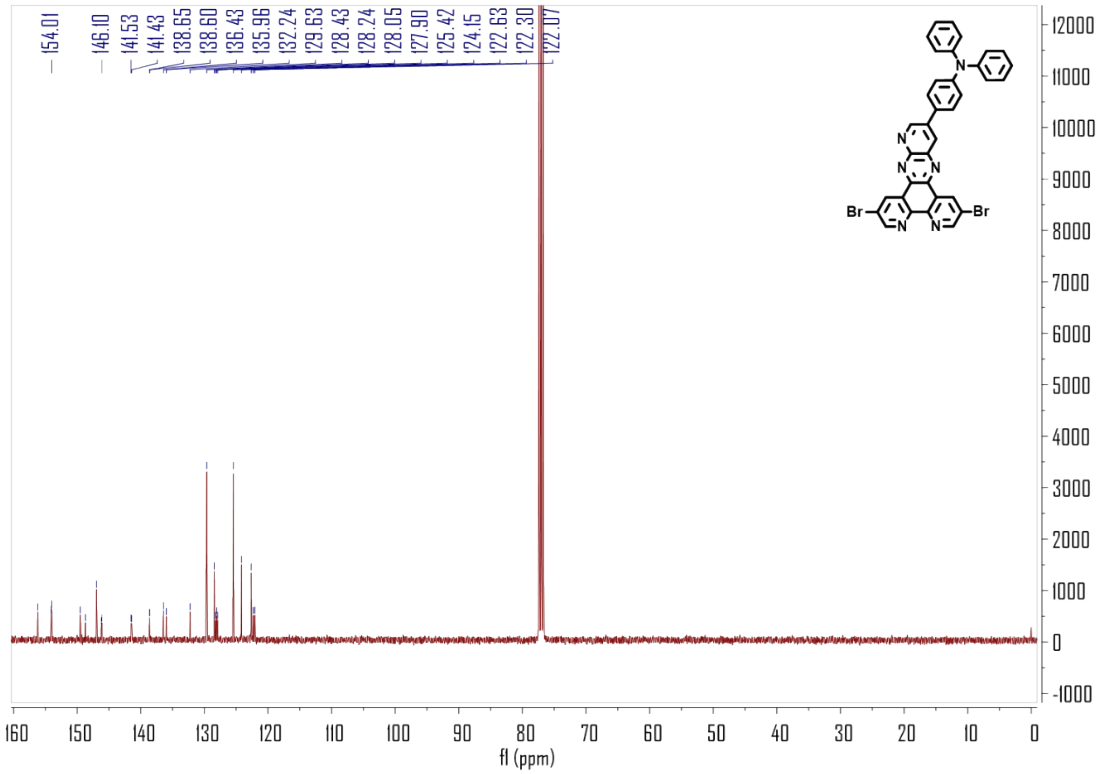

Figure S11. ^{13}C NMR spectrum of mTPA-PPP-2Br (400 MHz, $CDCl_3$).

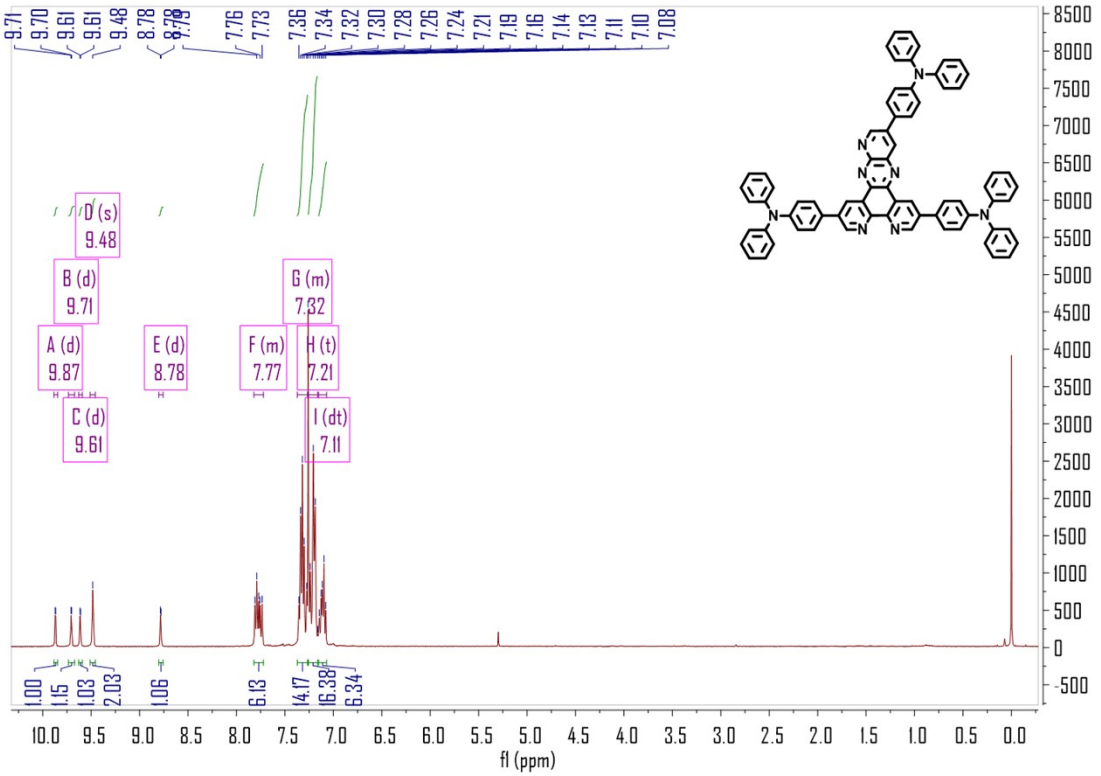

Figure S12. ^{1}H NMR spectrum of mtriTPA-PPP (400 MHz, $CDCl_3$).

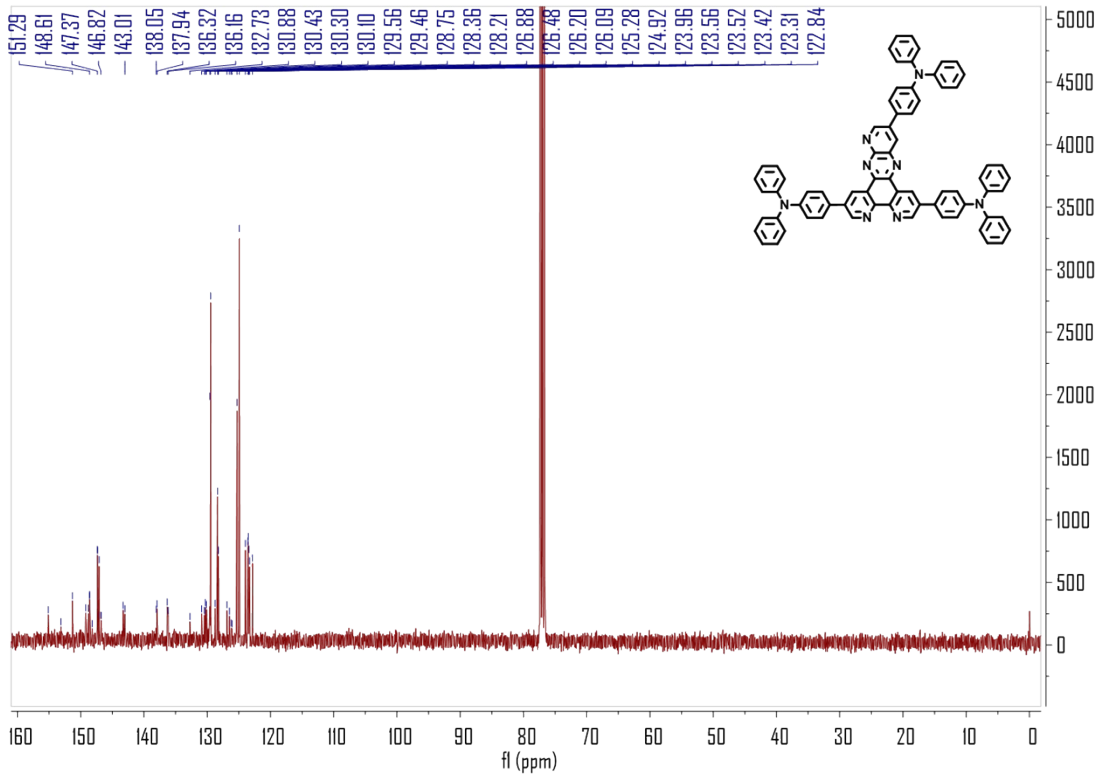

Figure S13. ^{13}C NMR spectrum of mtriTPA-PPP (400 MHz, $CDCl_3$).

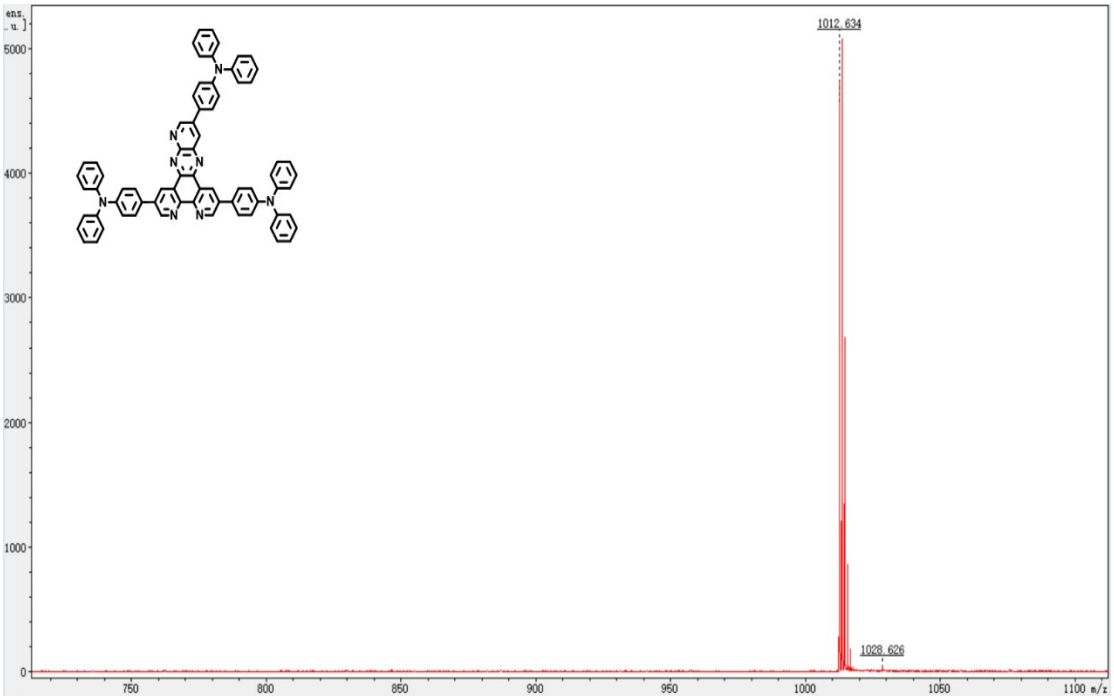

Figure S14. MALDI-TOF MS spectrum of mtriTPA-PPP.

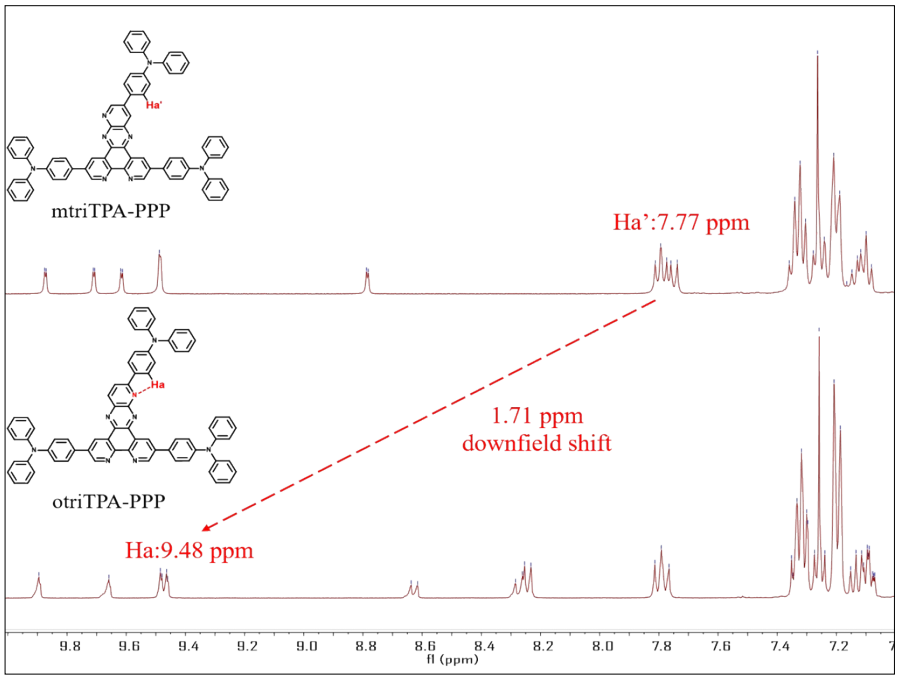

Figure S15. Comparison of ^{1}H NMR spectra of otriTPA-PPP and mtriTPA-PPP in $CDCl_3$ at room temperature.

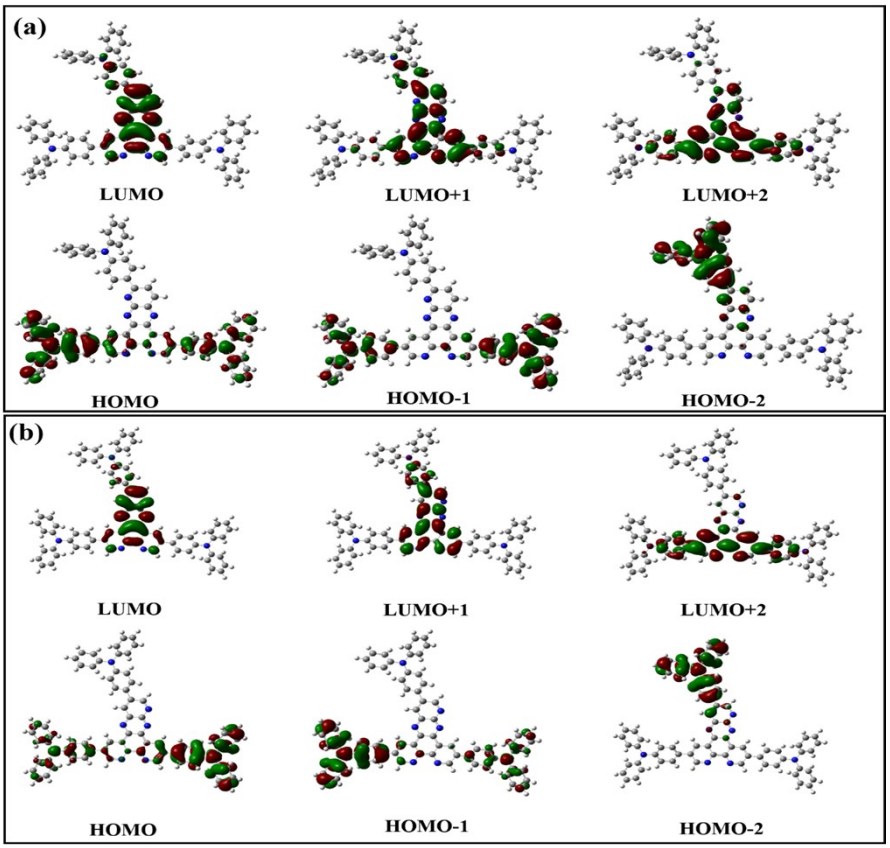

Figure S16. Quasi-degenerate unoccupied orbitals and quasi-degenerate occupied orbitals of otriTPA-PPP and mtriTPA-PPP.

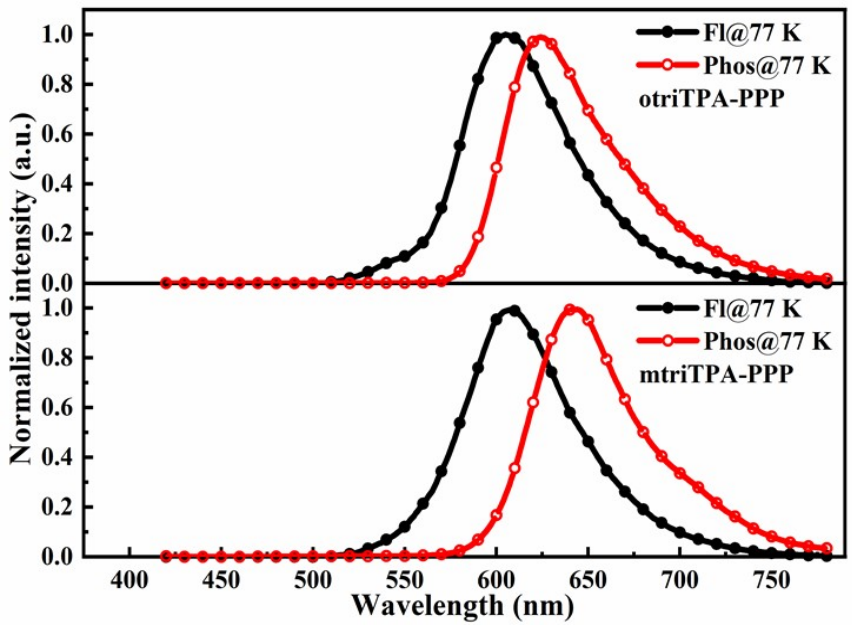

Figure S17. Fluorescence (Fl) and phosphorescence (Phos) spectra in in dilute toluene solution at 77 K.